Received: 6 March 2020 | Revised: 12 June 2020 | Accepted: 13 June 2020

DOI: 10.1002/pro.3903

PROTEIN STRUCTURE REPORTS

Solution structure of the zinc finger domain of human RNF144A ubiquitin ligase

Kazuhide Miyamoto | **Kaori Migita** | **Kazuki Saito**

Department of Pharmaceutical Health Care, Faculty of Pharmaceutical Sciences, Himeji Dokkyo University, Himeji, Hyogo, Japan

Correspondence
Kazuhide Miyamoto, Department of Pharmaceutical Health Care, Faculty of Pharmaceutical Sciences, Himeji Dokkyo University, Hyogo 670-8524, Japan.
Email: miyamoto@himeji-du.ac.jp

Funding information
Grant-in-Aid for Scientific Research, Grant/Award Number: 17K05942

Abstract

RNF144A is involved in protein ubiquitination and functions as an ubiquitin-protein ligase (E3) via its RING finger domain (RNF144A RING). RNF144A is associated with degradation of heat-shock protein family A member 2 (HSPA2), which leads to the suppression of breast cancer cell proliferation. In this study, the solution structure of RNF144A RING was determined using nuclear magnetic resonance. Moreover, using a metallochromic indicator, we spectrophotometrically determined the stoichiometry of zinc ions and elucidated that RNF144A RING binds two zinc atoms. This structural analysis provided the position and range of the active site of RNF144A RING at the atomic level, which contributes to the creation of artificial RING fingers having the specific ubiquitin-conjugating enzyme (E2)-binding capability.

KEYWORDS

artificial RING finger, E3 enzyme, NMR structure, RING finger, RNF144A, ubiquitination

1 | INTRODUCTION

Cross-braced motifs are found in various protein domains, such as RING,[1] PHD,[2] FYVE,[3] and ZZ[4] finger domains, which coordinate two zinc atoms in a cross-braced arrangement with eight ligands of Cys and/or His. Besides this common motif, each unique structure assumes an important biological function.[4] For example, most RING fingers in ubiquitination reaction function as ubiquitin (Ub)-protein ligases (E3s) which transfer activated Ub from Ub-conjugating (E2) enzymes to the substrate lysines.[5,6] RING fingers have a ββαβ compact fold[7] and specifically binds to E2s via its functional α region (active site).[1,8,9] In contrast, PHD, FYVE, and ZZ fingers are not involved in the ubiquitination system because they do not possess a functional helix region for E2-binding.[2,3,10] Previously, we proposed a design method for an artificial RING finger (ARF) that specifically binds to E2 enzymes and develops the auto-ubiquitination without a substrate. Such ARFs were created by transplanting active sites of RING fingers into other cross-brace zinc motifs (e.g., PHD fingers).[11–13] E2 activities, which are associated with leukemia,[14] breast cancer,[15,16] and gastric cancer,[17] are considered to be potential cancer biomarkers.[17] The ARF system enables the detection of the E2 activity during ubiquitination in the absence of the substrate.[16,18] Thus, the ARF method may lead to a screening system for E2 activities as a novel cancer diagnostic technique. The identification of appropriate positions for transplanting active sites is needed to extend the ARF method to various RING fingers. RNF144A functions as E3 via its RING finger domain (RNF144A RING). The ubiquitination of RNF144A is involved in the degradation of heat-shock protein family A member 2 (HSPA2) and leads to the suppression of breast cancer cell proliferation.[19] Therefore, in this study, the solution structure of RNF144A RING was elucidated using nuclear magnetic resonance (NMR). The determined RNF144A RING structure was compared with other RING finger structures.

2 | RESULTS AND DISCUSSION

2.1 | Zinc-binding stoichiometry of the RNF144A RING domain

The human RNF144A RING was synthesized using the standard Fmoc chemistry along the sequence (NP_001336110.1) shown in Figure 1a. Cysteine modification of 4-(2-pyridylazo) resorcinol (PAR) and *p*-hydroxymercuribenzoic acid (PHMB) clarified that the RNF144A RING peptide coordinates two zinc atoms.[20,21] The absorbance value (*A*) for the zinc-PAR complex of the RNF144A RING peptide was 0.31 at 500 nm. The concentration of the RNF144A RING peptide and bound zinc ions was 2.5 and 4.7 μM, respectively. Thus, the molar ratio [Zn]/[Peptide] was 1.9 at 20°C, indicating that the RNF144A RING peptide binds two zinc atoms.

2.2 | Chemical shift assignments and structural description

The ^{1}H, ^{13}C, and ^{15}N resonances for the $^{13}C/^{15}N$-labeled RNF144A RING peptide were assigned using conventional heteronuclear methods.[22] The backbone resonance assignments were completed except for the amide protons of Ala1 and Ala75. The methyl protons of Val and Leu in the prochiral center were stereospecifically assigned. The trans-conformation of all Pro was confirmed by the strong nuclear Overhauser effects (NOEs) between H^{α}(i-1) and H^{δ}(i) protons[23] and also by the $^{13}C^{\beta}$ and $^{13}C^{\gamma}$ chemical shift differences.[24] The C_{β} atoms of eight Cys residues (8, 11, 26, 28, 31, 34, 53, and 58) were identified as the zinc-binding ligands because their chemical shifts were between 27.0 and 32.0 ppm.[25] All the zinc-binding residues are highly conserved among the RNF144A RING homologs (Figure 1a). The NMR structure of RNF144A RING was determined based on 1,391 NOE distance constraints, 46 torsion angles constraints (φ, ψ), and 56 distance constraints for the tetrahedral zinc coordination. The structure calculations were performed by torsion angle dynamics on the program CYANA[26] and by the Smart Minimizer algorithm on the program Discovery Studio 2.1 (Accelrys Software Inc.).[13] The lowest-energy 20 structures in the well-ordered region (Cys8-Cys11, Met20-Ile23, Cys28-Gly46, Ala50-Pro54, Cys58-Lys60, and Gly62-Ala74) were superimposed over the backbone (N, C^{α}, and C′) atoms and the non-hydrogen atoms, with the r.m.s. deviations of 0.29 and 0.61 Å, respectively (Figure 1b). In a Ramachandran plot produced by the program PROCHECK-NMR,[27] 99.4% of the non-glycine residues were located in the most favored regions and additionally allowed regions as shown in Table 1. The secondary structures elements are two β-strands and two α-helices along the amino-acid sequence (β1: Met20-Thr21, β2: Phe30-Cys31, α1: Thr32-Glu45, and α2: Asn67-Cys71). The molecular surface model (Connolly's surface) of RNF144A RING was calculated with Discovery Studio 2.1 software (Figure 1c). Asp3, Lys9, Glu14, Lys36, Glu45, Glu48, and Lys60 residues were located on the surface of the molecule, and, on the opposite side, Glu18, Glu66, and Glu68 formed the negatively charged surface. The highly conserved residues (Leu10, Tyr38, and Pro54) formed a hydrophobic shallow groove on the surface, which was surrounded by the charged clusters. It was found that the RNF144A RING structure belongs to the C_4C_4-type RING structure, where two zinc-binding sites are formed by ZN1 (Cys8, Cys11, Cys31, and Cys34) and ZN2 (Cys26, Cys28, Cys53, and Cys58) in a cross-brace manner (Figure 1a,c). The residues Ile23, Phe30, Leu35, and Leu64 contributed to the formation of the structural core for proper folding of the RNF144A RING structure (Figure 2a). β1, β2, and α1 constitute the structural core, flanked by an additional α2 helix, which was stabilized by a hydrophobic cluster of Val39, Ile43, Leu51, Ile69, Met72, and Val73.

2.3 | Comparison with other RING domains

The RNF144A RING structure possesses an antiparallel β-sheet and two α-helical structures with a cross-braced zinc-binding arrangement. The typical RING fold from the c-Cbl protein (PDB ID: 1FBV) is a compact ββα (Figure 2b). However, the RNF144A RING structure adopts a ββαα arrangement, which is similar to that of the HHARI RING structure (PDB ID: 4KC9) as shown in Figure 2c. The c-Cbl RING and HHARI RING structures bind to E2s via their hydrophobic grooves formed by the residues (Ile383, Trp408, and Pro417) and (Ile188, Tyr215, and Pro232), respectively.[1,28] The determined RNF144A RING structure possesses a hydrophobic shallow groove formed by the structurally equivalent residues (Lue10, Tyr38, and Pro54) to those of other RINGs. By the Generative REgularized ModeLs of proteINs (GREMLIN) software, the conservation and coevolution patterns of the RNF144A family were calculated based on their sequences, and it was found that the highly conserved residues (Lue10, Tyr38, and Pro54) were crucial among the homologs (Figure 1). RING domains are classified into the four groups.[29] HHARI RING and c-Cbl RING belong to Group 2 and Group 3 of the RING family, respectively.[29] The structural alignments of the RNF144A RING structure, the HHARI RING structure, and the c-Cbl RING structure were shown in Figure 2d.

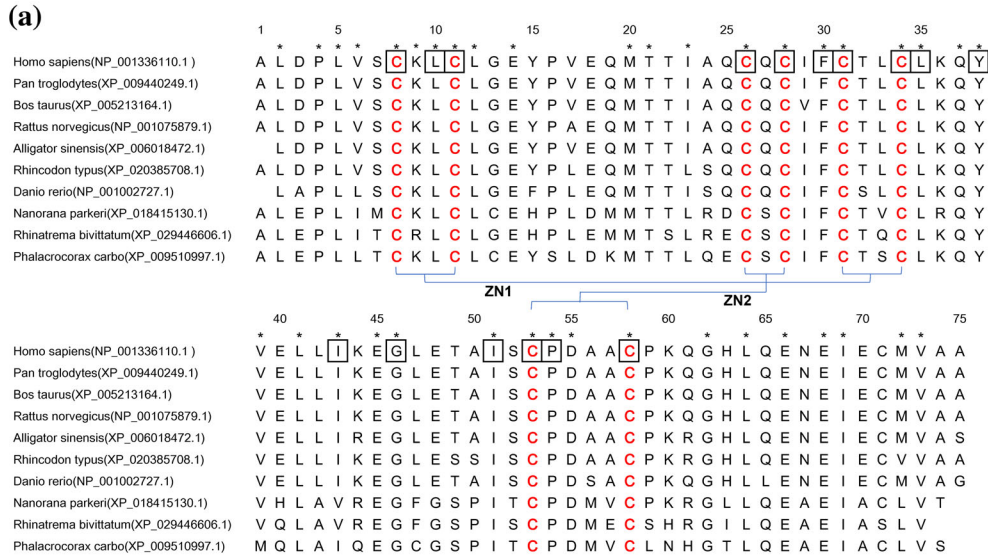

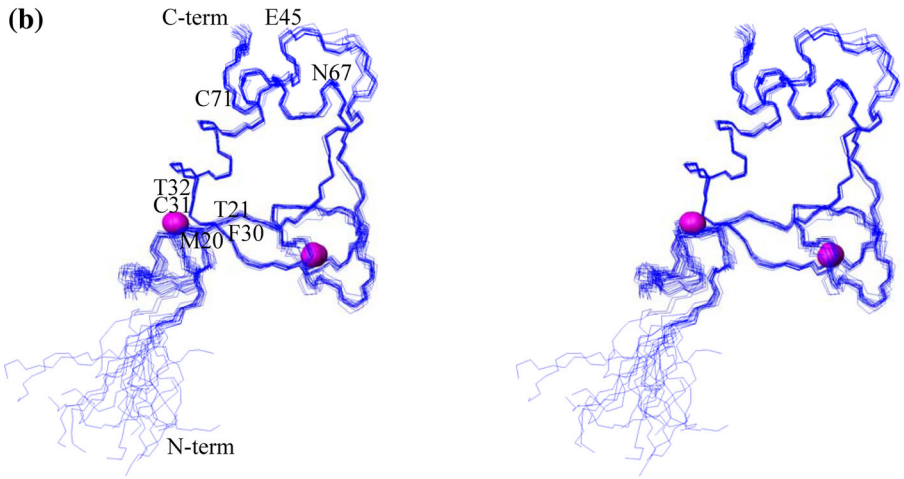

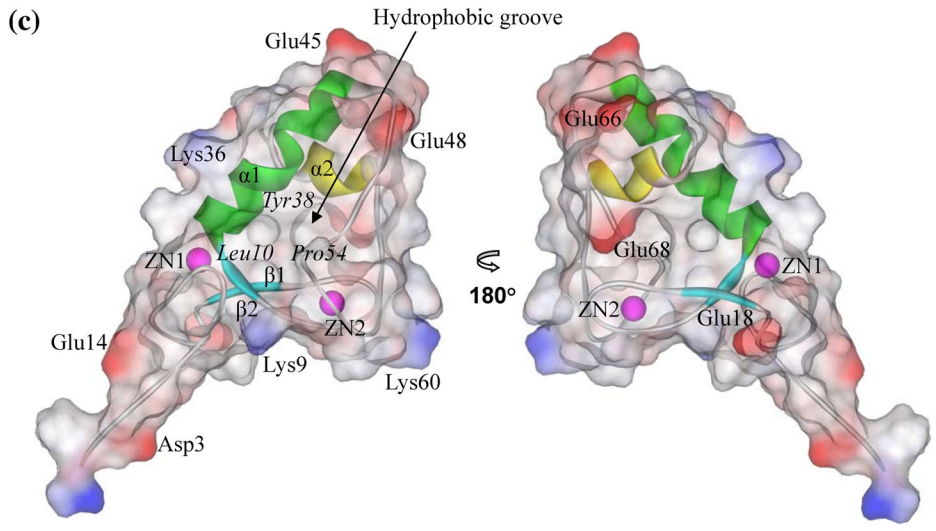

FIGURE 1 Sequence alignment and structural characteristics of RNF144A RING. (a) Sequence alignment of RING domains. Zinc-binding residues are shown in red. The two zinc-binding sites are ZN1 and ZN2 in a cross-brace arrangement. Stars indicate the highly conserved residues among homologs. The residues calculated by the program GREMLIN are boxed. (b) Stereoview of the best 20 structures superimposed on backbone atoms (residues Cys8-Cys11, Met20-Ile23, Cys28-Gly46, Ala50-Pro54, Cys58-Lys60, and Gly62-Ala74). The zinc atoms are colored in magenta. (c) The ribbon representation and the Connolly molecular surface of the lowest energy structure of RNF144A RING were shown with the electrostatic potential (blue, positive; red, negative). The hydrophobic groove is formed by residues (Leu10, Tyr38, and Pro54)

TABLE 1 Summary of structure statistics of RNF144A_RING[a]

NOE upper distance restraints	
Total	1,391
Short-range ($\|i-j\|=1$)	710
Medium range ($1<\|i-j\|<5$)	290
Long range ($\|i-j\|\geq 5$)	391
Dihedral angle restraints (φ and ψ)	46
Constraints for the zinc coordination (upper/lower)	28/28
CYANA target function value	0.02 Å^2
Distance constraints violations	
Number > 0.10 Å	0
Maximum	0.09 Å
PROCHECK Ramachandran plot analysis[b]	
Residues in most favored regions	63.2%
Residues in additionally allowed regions	36.2%
Residues in generously allowed regions	0.3%
Residues in disallowed regions	0.2%
RMS deviation to the average coordinates[b]	
Backbone atoms	0.29 Å
Heavy atoms	0.61 Å

[a]Except for the number of constraints, average values given for the set of 20 conformers with the lowest energy value.
[b]The values were calculated for residues 8–11, 20–23, 28–46, 50–54, 58–60 and 62–74.

In c-Cbl, Trp408 in the α1 region was considered significant as a specificity determinant for the E2-binding in ubiquitination,[1] whereas the structurally equivalent positions in RNF144A RING and HHARI RING were occupied by the residue Tyr, making the E2-binding interface for the HHARI/E2 complex structure.[28] Groups 1 and 4 have Trp and Leu in the structurally equivalent position of α1, respectively.[29] The conformation changes of the long Loop1 of HHARI RING, although shorter in Groups 1, 3, and 4, are induced to open its E2-binding surface and facilitate the complex formation between HHARI RING and E2.[28,29] HHARI RING binds to UbcH7/8 but not UbcH1/5.[30] The structure of RNF144A RING, which adopts the characteristic RING folding and the Loop1 region resembling those of HHARI RING, functions as an E3 ligase cooperating with UbcH7.[31] Thus, it was found that RNF144A RING is a member of Group 2 of the RING family. It is tempting to speculate that RNF144A RING promotes the ubiquitin chain elongation through its hydrophobic groove for E2-binding. The additional α2 helix of the Group 2 RING structure is located on the opposite surface from its E2-binding groove, and it is not included in the E2-binding interface.[28] Thus, the α2 helix of RNF144A RING is presumably irrelevant to its E2-binding partner recognition.

2.4 | Cross-brace structure for engineering an ARF

ARFs were designed by the transplanting method of the active sites of E3s, where cross-braced structures were used as a scaffold. The use of ARFs allows for the detection of E2 activities during ubiquitination without substrates.[18] It has been demonstrated that the ARF system is a novel technology for measuring E2 activities during ubiquitination in cancer cells, such as MCF7 breast cancer cells and acute promyelocytic leukemia-derived NB4 cells.[14,16] To extend the ARF strategy, the present work unveiled the position and the range of the active site of RNF144A RING at the atomic level. RNF144A RING belongs to the RING-in-between-RING family (RBR) of E3s. RBR is a subset found in >100 eukaryotic proteins[32] and is characterized by the presence of two RING domains (RING1 and RING2) separated by an IBR domain.[33] RNF144A RING is RING1, which is the characteristic domain of E3s.[31] Transplanting the active site of RNF144A RING onto other cross-brace zinc motifs will enable the creation of a novel ARF from the RBR family. Further ubiquitination assays of ARF/E2 will be needed to clarify the engineering methods of ARFs.

In conclusion, this report provided the first picture of the RING structure from the human RNF144A protein. The structure of the active site of RNF144A RING was elucidated at the atomic level, and thus, this report is useful information to enable the molecular design of ARFs, which might be used clinically as a cancer diagnostic technique.[17,34]

3 | METHODS

3.1 | Peptide synthesis

The sequence of RNF144A RING was produced using a SMART database search. The ^{13}C and ^{15}N-labeled peptide was uniformly synthesized with C-terminal amidation by the standard F-moc solid-phase method. Chemicals for peptide assembly, including amide resin, were purchased from Shimadzu Corp. (Kyoto, Japan) and Sigma-Aldrich Co. LLC (St. Louis, MO). After cleavage with trifluoroacetic acid, the peptide was applied to the purification system of reverse-phase HPLC with a Shim-pack C18 column (Shimadzu Corp.). The peptides were obtained as the purity >98% and its molecular mass was confirmed using MALDI-TOF MS on a Shimadzu AXIMA-TOF2. The RNF144A RING peptide was dissolved in 0.36 ml of 8 M guanidine–HCl and it was dialyzed overnight at 4°C against the degassed solution [20 mM Tris–HCl (pH 6.8), 50 mM NaCl, 1 mM

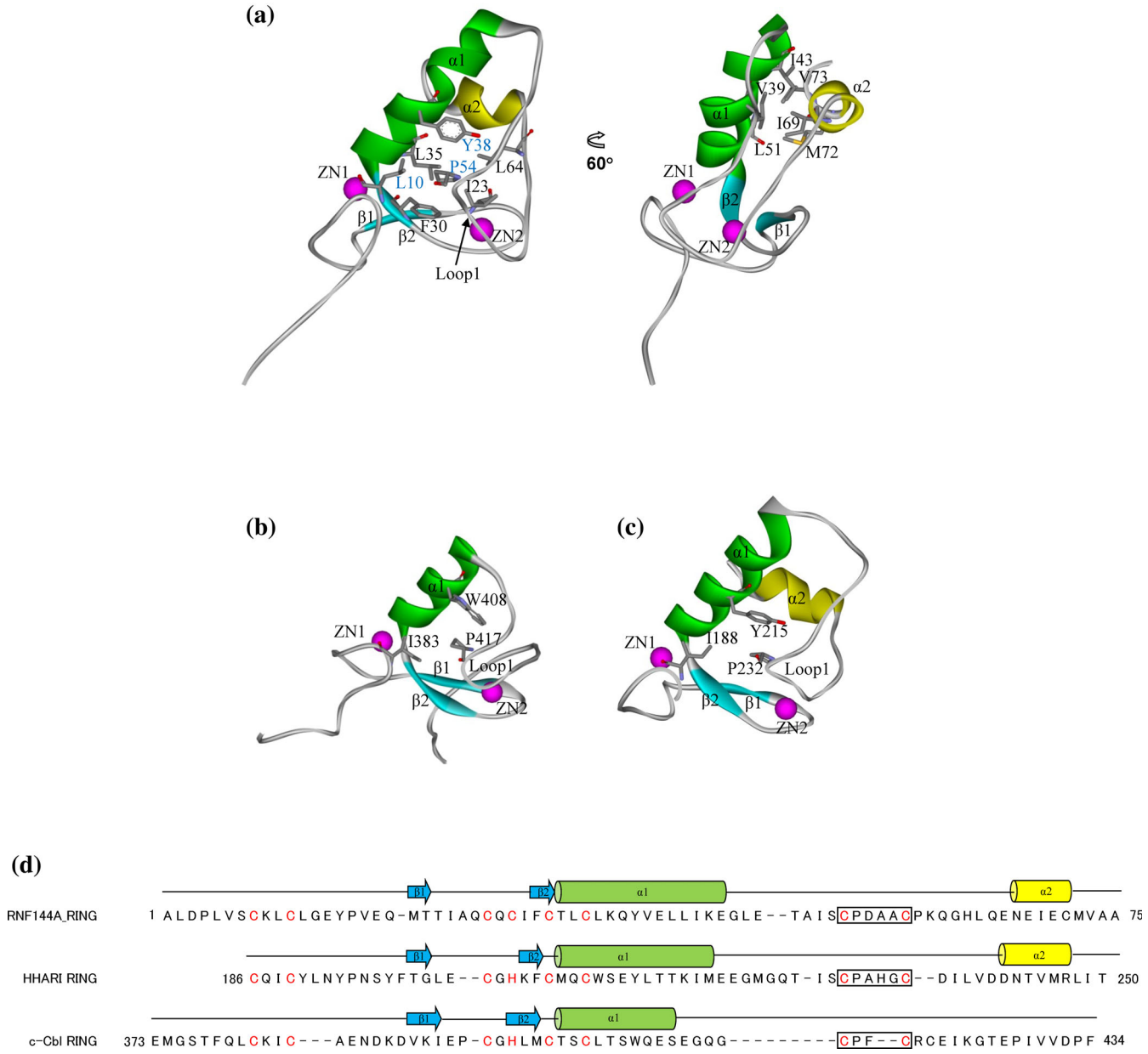

FIGURE 2 Structural comparisons of RNF144A RING and other RINGs. Ribbon diagrams of (a) the RNF144A RING structure, (b) the c-Cbl RING structure, and (c) the HHARI RING structure with the E2-binding residues, the Loop1 region, and zinc atoms (magenta). In RNF144A RING, the hydrophobic clusters and the putative E2-binding residues (blue) are shown with the heavy atoms. (d) Structural alignments of RNF144A RING, HHARI RING, and c-Cbl RING with secondary structure elements. Zinc ligands are indicated in red, and the residues for the Loop1 region are boxed

dithiothreitol, and 50 μM $ZnCl_2$] with a Slide-A-Lyzer Dialysis Cassette (PIERCE).[13]

3.2 | Quantitative determination of protein-binding zinc atoms

The concentration of the RNF144A RING peptide was spectrophotometrically estimated using the Bradford method with bovine serum albumin standard solution (Merck). The chemical modification of Cys residues was achieved by treatment with PHMB acid, thereby releasing Zn ions from the peptide. The amount of the Zn ions released was determined at 20°C by spectrophotometrically monitoring the formation of the zinc-PAR_2 complex at 500 nm using UV–visible spectrometer. The concentration of zinc ions released from the peptide was calculated by the equation $A = \varepsilon cl$, where the molar absorptivity (ε) is 6.6×10^4 M^{-1} cm^{-1}, the cell length (l) is 1.0 cm, and c represents the molecular concentration. Based on the molar ratio between the released Zn ions and the peptide, the content of the peptide-binding zinc ions was determined.[20,21]

3.3 | NMR spectroscopy

For NMR measurements, the peptide (1 mM) was dissolved in $^{1}H_2O/^{2}H_2O$ (9:1) in 20 mM Tris-d_{11}-HCl buffer (pH 6.9) (C/D/N Isotopes Inc., Canada) containing 50 mM NaCl, 1 mM 1,4-DL-dithiothreitol-d_{10}, and 50 μM $ZnCl_2$.[35,36] All NMR spectra were acquired at 298 K on a Bruker AVANCE 500 MHz equipped with a cryogenic probe and an AVANCE 800 spectrometer and then were processed using the program NMRPipe.[37] The backbone ^{1}H, ^{13}C, and ^{15}N resonances were assigned using triple-resonance experiments of HNCO, HN(CA)CO, HNCA, HN(CO)CA, HNCACB, and CBCA(CO)NH spectra.[22] Assignments of side chains were obtained from CCCONNH, HCCCONNH, HBHACONH, HCCH-COSY, HCCH-TOCSY, and CCH-TOCSY spectra. All NMR data were analyzed using the program NMRview.[38] Distance constraints were obtained from ^{15}N- and ^{13}C-edited NOESY-HSQC spectra using 80 ms mixing time.

3.4 | Structure determination

NOE peak lists of the NOESY spectra were generated as the input files by the peak picking and the automatic integration of the peak volume using NMRView. The three-dimensional structure was determined by automated NOE cross-peak assignments and structure calculations with torsion angle dynamics using the program CYANA 2.1.[26] The backbone dihedral constraints obtained by the program TALOS[39] were used. An error of ±30° was allowed for all the angle constraints. To maintain the tetrahedral bonding geometry of zinc atoms, the distance constraints (S^{γ}-S^{γ} distances of 3.7 ± 0.3 Å, C^{β}-Zn distances of 3.38 ± 0.13 Å, and S^{γ}-Zn distances of 2.35 ± 0.02 Å) were added into the NOE restraints with force constants of 500 kcal mol^{-1} $Å^{-1}$.[40,41] After initial calculations of 100 randomized conformers, structure calculations were carried out through the standard CYANA simulated annealing protocol with 10,000 torsion angle dynamics steps per conformer. Next, the 20 conformers obtained with the lowest CYANA target function values were chosen in the final calculations and then were subjected to energy minimization by the Smart Minimizer algorithm (Max steps 200, RMS gradient 0.01) on the Discovery Studio 2.1 software (Accelrys Software Inc.).[13] The structures were visualized and analyzed using the program MOLMOL.[42] By the program PROCHECK-NMR,[27] a Ramachandran plot of the structures was calculated and validated. Using the Discovery Studio 2.1 software, the Connolly molecular surface of the lowest energy structure was produced as solvent contact areas that were traced out by a probe molecule (water) with a radius of 1.4 Å.

3.5 | Protein data bank accession number

The 20 conformers of the RNF144A RING structure with the lowest energy in the final calculation were deposited in the Protein Data Bank (PDB entry 6L99).

ACKNOWLEDGMENTS

The authors would like to thank Dr. Yoshitsugu Shiro, from the RIKEN SPring-8 Center, for the NMR instrumentation. This research was supported by a Grant-in-Aid for Scientific Research (KAKENHI 17K05942).

CONFLICT OF INTEREST

The authors declare no potential conflict of interest.

AUTHOR CONTRIBUTIONS

Kazuhide Miyamoto: Conceptualization; data curation; formal analysis; funding acquisition; investigation; methodology; resources; supervision; validation; visualization; writing-original draft; writing-review and editing. **Kaori Migita:** Data curation; investigation; writing-review and editing. **Kazuki Saito:** Investigation; writing-review and editing.

ORCID

Kazuhide Miyamoto https://orcid.org/0000-0002-7792-0900

REFERENCES

1. Zheng N, Wang P, Jeffrey PD, Pavletich NP. Structure of a c-Cbl-UbcH7 complex: RING domain function in ubiquitin-protein ligases. Cell. 2000;102:533–539.
2. Pascual J, Martinez-Yamout M, Dyson HJ, Wright PE. Structure of the PHD zinc finger from human Williams-Beuren syndrome transcription factor. J Mol Biol. 2000;304:723–729.
3. Misra S, Hurley JH. Crystal structure of a phosphatidylinositol 3-phosphate-specific membrane-targeting motif, the FYVE domain of Vps27p. Cell. 1999;97:657–666.
4. Legge GB, Martinez-Yamout MA, Hambly DM, et al. ZZ domain of CBP: An unusual zinc finger fold in a protein interaction module. J Mol Biol. 2004;343:1081–1093.
5. Lorick KL, Jensen JP, Fang S, Ong AM, Hatakeyama S, Weissman AM. RING fingers mediate ubiquitin-conjugating enzyme (E2)-dependent ubiquitination. Proc Natl Acad Sci U S A. 1999;96:11364–11369.
6. Weissman AM. Themes and variations on ubiquitylation. Nat Rev Mol Cell Biol. 2001;2:169–178.
7. Borden KL. RING domains: Master builders of molecular scaffolds? J Mol Biol. 2000;295:1103–1112.

8. Brzovic PS, Rajagopal P, Hoyt DW, King MC, Klevit RE. Structure of a BRCA1-BARD1 heterodimeric RING-RING complex. Nat Struct Biol. 2001;8:833–837.
9. Katoh S, Tsunoda Y, Murata K, Minami E, Katoh E. Active site residues and amino acid specificity of the ubiquitin carrier protein-binding RING-H2 finger domain. J Biol Chem. 2005; 280:41015–41024.
10. Scheel H, Hofmann K. No evidence for PHD fingers as ubiquitin ligases. Trends Cell Biol. 2003;13:285–287. author reply 287-288.
11. Miyamoto K, Togiya K. The creation of the artificial RING finger from the cross-brace zinc finger by alpha-helical region substitution. Biochem Biophys Res Commun. 2010;394: 972–975.
12. Miyamoto K. Ubiquitination of an artificial RING finger without a substrate and a tag. J Pept Sci. 2012;18:135–139.
13. Miyamoto K. Structural model of ubiquitin transfer onto an artificial RING finger as an E3 ligase. Sci Rep. 2014;4:6574.
14. Miyamoto K, Sumida M, Yuasa-Sunagawa M, Saito K. Highly sensitive detection of E2 activity in ubiquitination using an artificial RING finger. J Pept Sci. 2017;23:222–227.
15. Wu X, Zhang W, Font-Burgada J, et al. Ubiquitin-conjugating enzyme Ubc13 controls breast cancer metastasis through a TAK1-p38 MAP kinase cascade. Proc Natl Acad Sci U S A. 2014;111:13870–13875.
16. Miyamoto K, Nakatani A, Sunagawa M, Saito K. Unique autoubiquitination activities of artificial RING fingers in cancer cells. Protein Sci. 2018;27:1704–1709.
17. Yang M, Qu Y, Shi R, et al. Ubiquitin-conjugating enzyme UbcH10 promotes gastric cancer growth and is a potential biomarker for gastric cancer. Oncol Rep. 2016;36:779–786.
18. Miyamoto K, Saito K. Concise machinery for monitoring ubiquitination activities using novel artificial RING fingers. Protein Sci. 2018;27:1354–1363.
19. Yang YL, Zhang Y, Li DD, et al. RNF144A functions as a tumor suppressor in breast cancer through ubiquitin ligase activity-dependent regulation of stability and oncogenic functions of HSPA2. Cell Death Differ. 2020;27:1105–1108.
20. Hunt JB, Neece SH, Ginsburg A. The use of 4-(2-pyridylazo)resorcinol in studies of zinc release from *Escherichia coli* aspartate transcarbamoylase. Anal Biochem. 1985;146:150–157.
21. Shang Z, Liao YD, Wu FY, Wu CW. Zinc release from Xenopus transcription factor IIIA induced by chemical modifications. Biochemistry. 1989;28:9790–9795.
22. Clore GM, Gronenborn AM. Multidimensional heteronuclear nuclear magnetic resonance of proteins. Methods Enzymol. 1994;239:349–363.
23. Wüthrich K. NMR with Proteins and Nucleic Acids. NMR of proteins nucleic acids. New York: John Wiley, 1986.
24. Schubert M, Labudde D, Oschkinat H, Schmieder P. A software tool for the prediction of Xaa-Pro peptide bond conformations in proteins based on 13C chemical shift statistics. J Biomol NMR. 2002;24:149–154.
25. Kornhaber GJ, Snyder D, Moseley HN, Montelione GT. Identification of zinc-ligated cysteine residues based on 13Calpha and 13Cbeta chemical shift data. J Biomol NMR. 2006;34: 259–269.
26. Guntert P. Automated NMR structure calculation with CYANA. Methods Mol Biol. 2004;278:353–378.
27. Laskowski RA, Rullmannn JA, MacArthur MW, Kaptein R, Thornton JM. AQUA and PROCHECK-NMR: Programs for checking the quality of protein structures solved by NMR. J Biomol NMR. 1996;8:477–486.
28. Yuan L, Lv Z, Atkison JH, Olsen SK. Structural insights into the mechanism and E2 specificity of the RBR E3 ubiquitin ligase HHARI. Nat Commun. 2017;8:211.
29. Katoh S, Hong C, Tsunoda Y, et al. High precision NMR structure and function of the RING-H2 finger domain of EL5, a rice protein whose expression is increased upon exposure to pathogen-derived oligosaccharides. J Biol Chem. 2003;278:15341–15348.
30. Moynihan TP, Ardley HC, Nuber U, et al. The ubiquitin-conjugating enzymes UbcH7 and UbcH8 interact with RING finger/IBR motif-containing domains of HHARI and H7-AP1. J Biol Chem. 1999;274:30963–30968.
31. Ho SR, Lee YJ, Lin WC. Regulation of RNF144A E3 ubiquitin ligase activity by self-association through its transmembrane domain. J Biol Chem. 2015;290:23026–23038.
32. van der Reijden BA, Erpelinck-Verschueren CA, Lowenberg B, Jansen JH. TRIADs: A new class of proteins with a novel cysteine-rich signature. Protein Sci. 1999;8:1557–1561.
33. Capili AD, Edghill EL, Wu K, Borden KL. Structure of the C-terminal RING finger from a RING-IBR-RING/TRIAD motif reveals a novel zinc-binding domain distinct from a RING. J Mol Biol. 2004;340:1117–1129.
34. Xie C, Powell C, Yao M, Wu J, Dong Q. Ubiquitin-conjugating enzyme E2C: A potential cancer biomarker. Int J Biochem Cell Biol. 2014;47:113–117.
35. Miyamoto K, Togiya K, Kitahara R, Akasaka K, Kuroda Y. Solution structure of LC5, the CCR5- derived peptide for HIV-1 inhibition. J Pept Sci. 2010;16:165–170.
36. Miyamoto K, Togiya K. Solution structure of LC4 transmembrane segment of CCR5. PLoS One. 2011;6:e20452.
37. Delaglio F, Grzesiek S, Vuister GW, Zhu G, Pfeifer J, Bax A. NMRPipe: A multidimensional spectral processing system based on UNIX pipes. J Biomol NMR. 1995;6:277–293.
38. Johnson BA. Using NMRView to visualize and analyze the NMR spectra of macromolecules. Methods Mol Biol. 2004;278:313–352.
39. Cornilescu G, Delaglio F, Bax A. Protein backbone angle restraints from searching a database for chemical shift and sequence homology. J Biomol NMR. 1999;13:289–302.
40. Wang B, Alam SL, Meyer HH, et al. Structure and ubiquitin interactions of the conserved zinc finger domain of Npl4. J Biol Chem. 2003;278:20225–20234.
41. Tamames B, Sousa SF, Tamames J, Fernandes PA, Ramos MJ. Analysis of zinc-ligand bond lengths in metalloproteins: Trends and patterns. Proteins. 2007;69:466–475.
42. Koradi R, Billeter M, Wuthrich K. MOLMOL: A program for display and analysis of macromolecular structures. J Mol Graph. 1996;14(51–55):29–32.

How to cite this article: Miyamoto K, Migita K, Saito K. Solution structure of the zinc finger domain of human RNF144A ubiquitin ligase. *Protein Science*. 2020;29:1836–1842. https://doi.org/10.1002/pro.3903